Applied Thermal Engineering 88 (2015) 315–321

Contents lists available at ScienceDirect

Applied Thermal Engineering

journal homepage: www.elsevier.com/locate/apthermeng

Unidirectional freezing of phase change materials saturated in open-cell metal foams

Shangsheng Feng [a, b], Ye Zhang [c], Meng Shi [c], Ting Wen [a], Tian Jian Lu [a, b, *]

[a] Multidisplinary Research Center for Lightweight Structures and Materials, Xi'an Jiaotong University, Xi'an 710049, PR China
[b] State Key Laboratory of Mechanical Structure Strength and Vibration, School of Aerospace, Xi'an Jiaotong University, Xi'an 710049, PR China
[c] School of Energy and Power Engineering, Xi'an Jiaotong University, Xi'an 710049, PR China

HIGHLIGHTS

- Unidirectional freezing of water as a PCM embedded in metal foams was studied.
- Local thermal equilibrium between a metal foam and PCM was experimentally observed.
- The one-equation model suffices to model the PCM-saturated metal foams.
- Thermal contact resistance has negligible influence on freezing rates.
- Thus, one can simply embed metal foams into PCMs with no need for interface bonding.

ARTICLE INFO

Article history:
Received 17 June 2014
Received in revised form
22 August 2014
Accepted 20 September 2014
Available online 30 September 2014

Keywords:
Metal foam
Phase change material
Contact resistance
Local thermal equilibrium

ABSTRACT

An experimental and theoretical study of the unidirectional freezing of water as a PCM filled in metal foams has been carried out. Particular concern is placed upon determining how the contact conditions between the metal foam and the cold wall influence the freezing process, as well as exploring the local thermal equilibrium between the metal foam and the PCM. To address these questions, three contact conditions were considered, *i.e.*, natural contact, applied pressure, and bonding with a high thermal conductivity adhesive. To explore the local thermal equilibrium, temperatures on foam ligaments and within the pores were measured individually using thermocouples. For the current copper foam/water PCM system, the three different contact conditions were found to have similar freezing rate. This indicates that in practice one can simply embed metal foam blocks into PCMs with no need of bonding them to the cold wall *via* sintering, thermal adhesive or other methods, thereby reducing the costs of devices in thermal energy storage systems. Effects of foam properties, including porosity and pore density on the freezing rate, were also discussed.

1. Introduction

Phase change materials (PCMs) have the capability of storing and releasing sizeable latent heat upon solid–liquid phase transition. They have been widely used in many applications such as thermal management of electronics, heat protection systems in aerospace applications, and thermal energy storage. Various organic and inorganic materials with a wide range of melting temperatures can be used as potential PCMs for different applications. PCMs with a low melting temperature (less than 20 °C) are mainly used for *cold energy storage*, e.g., food storage and air conditioning [1], while PCMs with a higher melting temperature can be used for *heat energy storage*, e.g., waste heat recovery systems, buildings, and solar power plants [2]. However, most PCMs suffer from low thermal conductivity, which limits attainable heat transfer rates thus prolonging energy charging and discharging periods. Thermal conductivity enhancement of PCMs has therefore been studied extensively, as documented in several recent review papers [1,3,4].

Existing methods for enhancing the thermal conductivity of PCMs may be divided into two broad categories: 1) dispersing nano-sized additives into PCMs to produce *free-form and fluid-like composites* and 2) introducing *fixed high-conductivity inserts*. Various nanoparticle-enhanced PCMs such as CuO-cyclohexane [5], Cu-paraffin [6] and Al_2O_3–H_2O [7] have been studied and have

* Corresponding author. State Key Laboratory of Mechanical Structure Strength and Vibration, School of Aerospace, Xi'an Jiaotong University, Xi'an 710049, PR China.
E-mail addresses: shangshengf@gmail.com (S. Feng), tjlu@mail.xjtu.edu.cn (T.J. Lu).

http://dx.doi.org/10.1016/j.applthermaleng.2014.09.055
1359-4311/

Nomenclature

c_s	heat capacity of copper (J/kg K)
$c_{PCM,l}$	heat capacity of water (J/kg K)
$c_{PCM,s}$	heat capacity of ice (J/kg K)
H	height of metal foams along freezing direction (m)
$k_{ef,l}$	effective thermal conductivity of foam/water composite (W/mK)
$k_{ef,s}$	effective thermal conductivity of foam/ice composite (W/mK)
$k_{PCM,l}$	thermal conductivity of water (W/mK)
$k_{PCM,s}$	thermal conductivity of ice (W/mK)
L	latent heat (J/kg)
s	growth of ice thickness (m)
T_i	initial temperature (K)
T_m	freezing temperature (K)
T_0	cold wall temperature (K)

Greek symbols

ρ_s	density of copper (kg/m^3)
$\rho_{PCM,l}$	density of water (kg/m^3)
$\rho_{PCM,s}$	density of ice (kg/m^3)
ε	porosity
δ	thickness of sub-layer PCM (m)

shown reduced freezing/melting times relative to those of the pure base material. However, the phase change process is not enhanced monotonously by an increase in the concentration of nanoparticles due to precipitation of particles [5]. The problem of particle precipitation can be alleviated by using *fixed high-conductivity inserts*. Copper, aluminum, nickel, stainless steel and carbon in various forms (e.g., fins [8], honeycomb [9], brush [10], foam [2], and graphite [11]) have been utilized as fixed inserts. Upon extensive review of state of the art enhancement methods, Fernandes et al. [4] argued that embedment of open-cell metal foams in PCMs is one of the most promising approaches to enhancing thermal conductivity and heat transfer rates, as metal foams prove to be a non-expensive, easy to handle and are abundantly available. Zhao et al. [2] experimentally investigated the melting and solidification processes of paraffin wax RT 58 embedded in copper foams and found that the addition of metal foams can increase the overall heat transfer rate by 3–10 times during the melting process and reduce the solidification time by more than half. The feasibility of using metal foams and graphite to enhance the heat transfer of $NaNO_3$ as a PCM for high temperature solar thermal energy storage was experimentally studied by Zhao and Wu [12], and the overall performance of metal foam inclusion was found to be superior to expanded graphite inclusion.

Modelling heat transfer in a porous medium, e.g., a PCM-metal foam composite, can be performed with either a one- or two-equation model, depending on whether local thermal equilibrium is assumed between the two phases of the filled porous medium. A one-equation model assumes local thermal equilibrium, i.e., the foam and the fluid have an identical temperature. The two-equation model assumes local thermal non-equilibrium, i.e., the foam and the fluid have different temperatures, and each constituent is characterized with a separate equation. Based upon the assumption of local thermal non-equilibrium, Mesalhy et al. [13] numerically studied the melting process of PCMs saturated in metal foams within an annular space. Tian and Zhao [14] and Li et al. [15] also adopted the two-equation model to simulate the melting process of paraffin/metal foams composite under horizontal and vertical positions, respectively. By comparing the prediction results from the one-equation model and the two-equation model, Krishnan et al. [16] revealed that when the interstitial Nusselt number between the foam and the solid-/fluid-layer of PCM exceeds a certain value, the local thermal equilibrium assumption is valid. Recently, Hu and Patnalk [17] applied two different simulation methodologies for paraffin-embedded aluminum foam: one was direct numerical simulation (DNS), which makes no assumptions regarding local thermal equilibrium; the other was a volume averaged simulation using both one- and two-equation models. Upon comparing results from the two methodologies, the volume averaged simulation was found to be sufficient for modelling the paraffin/aluminum foam composite.

Although solid–liquid phase change in metal foams has been extensively studied, there are still several areas that need to be addressed. First, there is no experimental investigation on the local thermal situation between metal foams and PCMs. A two-equation model, which was used in most previous studies, involves empirical parameters (e.g., an interstitial heat transfer coefficient), which introduce uncertainties into model predictions. Meanwhile, if the actual thermal situation is close to local thermal equilibrium, a one-equation model, requiring no interstitial heat transfer coefficients for closure, is more adequate and simple. Therefore, a proper understanding of local thermal equilibrium is needed to select the appropriate model to achieve accurate model prediction. Furthermore, the influence of the contact condition between a metal foam and a heat transfer surface on phase change heat transfer has not been covered in previous studies.

To address the above issues, unidirectional freezing of water (a common phase change material in cold energy storage [1,11]) embedded in open-cell copper foams was investigated both experimentally and theoretically. The problem is depicted in Fig. 1. The distilled water had an initial temperature of T_i, higher than the freezing temperature T_m. At time $t = 0$, the temperature of the cold wall ($x = 0$) was suddenly reduced to T_0 ($<T_m$) and subsequently held constant. At $x = H$, the boundary condition was assumed adiabatic. Three copper foam samples were tested with three different contact conditions between the foam and the cold wall: natural contact, applied pressure, and bonding with a high thermal conductivity adhesive. Propagation of the freezing front in different test cases was recorded using a digital camera. To explore local thermal equilibrium between the foam and the PCM, temperatures of the foam ligaments and within the pores were separately recorded with thermocouples. The effects of foam properties upon freezing were also analysed in detail.

2. Experimental setup and procedures

A test rig was designed and built to investigate quasi one-dimensional freezing of PCMs saturated in open-cell copper

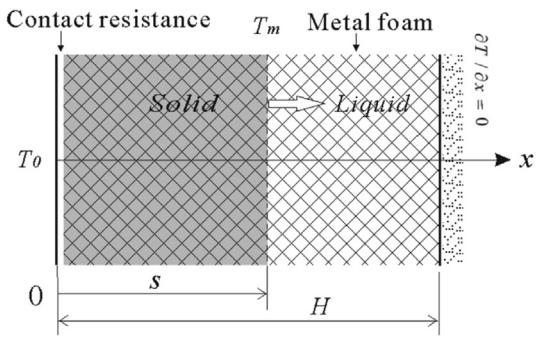

Fig. 1. Unidirectional freezing of PCMs saturated in metal foams.

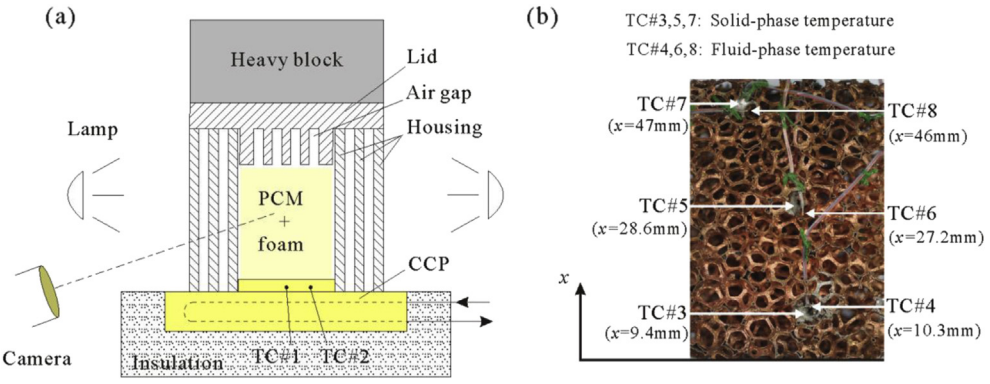

Fig. 2. Experimental details: (a) Schematic diagram of the apparatus for unidirectional freezing experiment; (b) Arrangement of thermocouples.

foams with distilled water selected as the PCM. As schematically shown in Fig. 2(a), cooling was provided from the bottom, i.e., the freezing front propagated upward. Thus, natural convection in the water was suppressed to ensure unidirectional freezing.

The housing of the PCM/foam composite was fabricated from transparent Perspex tubing (thermal conductivity k ~ 0.2 W/mK) with a 30 × 40 mm^2 inner cross-section and with two layers of air gaps (gap thickness = 1 mm). As shown schematically in Fig. 2(a), the multi-layer air gaps prevented heat loss from the side surfaces of the housing. For additional thermal insulation, the four side surfaces of the housing were wrapped with insulation cotton, while the top surface was covered by a fin-like lid made of Perspex. The air gaps between adjacent fins in the lid provided an insulated boundary as well as a reserved space to accommodate possible volume expansion upon phase change. Sufficient insulation at the side and top surfaces of the housing is important to ensure one-dimensional freezing. Because experiments were performed during a cold winter (room temperature ~12 °C), it was estimated that the heat entering into the housing from the side and top surfaces was less than 5.6% of the total released energy of the PCM to the cold wall at the end of the freezing process. A heavy block, 20 kg in weight, was placed on the lid to provide a nominal contact pressure of 0.16 MPa between the foam and the cold wall. Note that this pressure was not enough to result in macroscopic deformation of the foam, which would change the porosity of the foam.

For freezing front visualization, the insulation of the front and side surfaces of the housing were periodically removed. As shown in Figs. 2(a) and 3, two lamps placed near the side surfaces of the housing were also periodically turned on to more clearly illuminate the freezing front. Images were captured every 10 or 20 min for a time period of approximately 10 s. Accordingly, the front or side housing insulation was only removed for approximately 1% of the total freezing time. Therefore, heating from the lamps can be ignored. To determine the location of the freezing front in the images, a Kapton sheet with a printed scale was attached to the inner surface of the housing tube (see Fig. 3) so that the freezing front could be observed at the same surface as the scale. During measurements, it was important to ensure proper alignment to avoid errors caused by a non-perpendicular view angle.

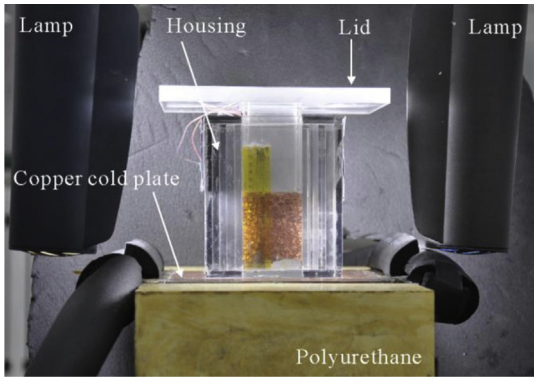

Fig. 3. Experimental apparatus.

Before mounting the housing tube on a copper cold plate (CCP) at the bottom, a thin layer of sealant was spread on the exposed surface of the CCP to prevent any leakage of water from the tube. The CCP was designed with embedded flow passages to ensure a constant cold temperature boundary condition. Flow passages were connected to the inlet and outlet ports of an isothermal bath with a temperature stability of 0.01 °C and the pumping rate was fixed at 6 L/min. A 1:1 water/ethylene glycol mixture with a freezing point of approximately −34 °C was used as the working fluid in the isothermal bath to maintain a CCP temperature below the ice point (0 °C). A small copper block of size 30 × 40 × 4 mm^3 was bonded to the CCP using a thermal adhesive, which served as a pedestal for the PCM/foam composite. To evaluate the temperature uniformity, two slots (cross-sectional size: 1 × 1 mm^2) were cut from the lower surface of the copper block to accommodate thermocouples, as denoted by TC#1 and TC#2 in Fig. 2(a), with TC#1 positioned at the centre of the copper block and TC#2 at the corner. Due to low thermal resistance of the copper block, the temperatures measured by TC#1 and TC#2 represent the cold wall temperature, *i.e.*, T_0, as shown in Fig. 1. During the steady state, the average temperature of TC#1 and TC#2 was found to be approximately 0.6 °C higher than the setting temperature (−9 °C) in the isothermal bath. This small temperature difference indicates good thermal insulation of the CCP and the piping.

To investigate the local thermal equilibrium between the metal foam and PCM, three pairs of T-type thermocouples (Omega, wire diameter: 0.127 mm), *i.e.*, (TC#3, TC#4), (TC#5, TC#6) and (TC#7, TC#8) as marked in Fig. 2(b), were used to measure temperature variations of the foam and PCM at three different vertical locations. The thermocouple beads of TC#3, TC#5 and TC#7 were attached to the foam ligament using thermal adhesive, whereas the beads of TC#4, TC#6, and TC#8 were located within the corresponding pore space close to TC#3, TC#5, and TC#7, respectively. The coordinates of each thermocouple bead are shown in Fig. 2(b). All of the thermocouples were connected to a data acquisition system (Agilent, 34970) for temperature recording. The uncertainty of the T-type thermocouples associated with the data acquisition system was estimated to be 0.2 °C by testing the temperature of the ice water mixture.

Three open-cell copper foam samples with selected pore densities (measured by PPI, or pores per inch) and different porosities were tested, as shown in Fig. 4. Sample 1 had a pore density of 8 PPI and a porosity of 0.96; sample 2 had the same pore density as

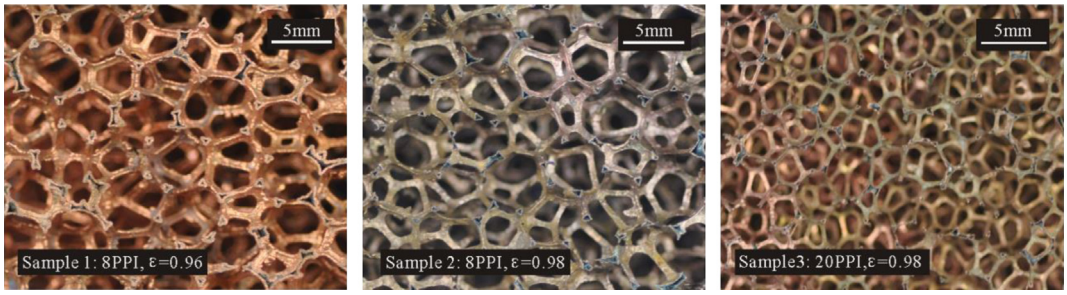

Fig. 4. Copper foam samples with different pore densities and porosities.

sample 1 but a higher porosity of 0.98; sample 3 had the same porosity as sample 2 but a higher pore density of 20 PPI. The pore density of each sample was provided by the supplier, while the porosity was measured by weighing the sample. Each sample had an overall size of 30 × 40 × 50 (height) mm^3.

Six test cases with different contact conditions between the foam and the cold wall were considered, as specified in Table 1. Case 1 served as reference, *i.e.*, freezing of distilled water without metal foams. Cases 2–4 were tested using sample 1 with three different contact conditions: In case 2, the sample was positioned on the copper block without an external contact force; in case 3, a 20 kg metal block was placed on the lid to provide contact pressure; in case 4, the sample was bonded to the cold wall using a high thermal conductivity adhesive (Arctic Silver™, $k > 8.8$ W/mK). Cases 5 and 6 were tested using sample 2 and sample 3, respectively, under the natural contact condition. The initial temperature of the water was approximately 12.4 °C for each test case. Given the huge latent heat of water relative to its sensible heat capacity, the small differences in initial temperatures of the six test cases should have negligible influence on the freezing rate.

3. Theory

To explore the effect of contact conditions and local thermal equilibrium from a theoretical point of view, a numerical model was developed for one-dimensional freezing of PCMs saturated in open-cell metal foams. To evaluate the effect of contact conditions, a thin sub-layer of PCM having a thickness of δ between the foam and the cold wall was included in the model, as shown in Fig. 5. Local thermal equilibrium between metal foam and PCM was assumed at the pore level, so that the one-equation model could be adopted for the modelled copper foam/PCM composite.

Based on the above assumptions, the volume-averaged governing equation for the metal foam/PCM composite as well as the PCM sub-layer of Fig. 5 may be written as:

$$\left\{\varepsilon\left[\rho_{\mathrm{PCM},l}c_{\mathrm{PCM},l}(1-f)+\rho_{\mathrm{PCM},s}c_{\mathrm{PCM},s}f\right]+(1-\varepsilon)\rho_s c_s\right\}\frac{\partial T}{\partial t}$$
$$=\left[\left(1-f\right)k_{\mathrm{ef},l}+fk_{\mathrm{ef},s}\right]\frac{\partial^2 T}{\partial x^2}-\frac{\partial\left[\rho_{\mathrm{PCM},s}L\varepsilon(1-f)\right]}{\partial t} \quad (1)$$

Table 1
Summary of test cases.

Case no.	Sample no.	Foam characteristics	Initial temperature	Contact condition
1	W/O	Without foam	12.4 °C	W/O
2	1	8 PPI, $\varepsilon = 0.96$	12.4 °C	Natural contact
3	1	8 PPI, $\varepsilon = 0.96$	13.1 °C	20 kg block
4	1	8 PPI, $\varepsilon = 0.96$	12.8 °C	Thermal glue
5	2	8 PPI, $\varepsilon = 0.98$	12.9 °C	Natural contact
6	3	20 PPI, $\varepsilon = 0.98$	12.4 °C	Natural contact

where $\rho_{\mathrm{PCM},l}$, $c_{\mathrm{PCM},l}$ are density and specific heat of water; $\rho_{\mathrm{PCM},s}$, $c_{\mathrm{PCM},s}$ are density and specific heat of ice; and ρ_s, c_s are density and specific heat of the base material of the metal foam. ε is the porosity of metal foam. $k_{\mathrm{ef},l}$ and $k_{\mathrm{ef},s}$ are effective thermal conductivities of foam/water and foam/ice composites, respectively. f is the solid fraction, which was updated according to the computed temperature, as:

$$f=\begin{cases}0 & T>T_{\mathrm{liquidus}}\\ \dfrac{T_{\mathrm{liquidus}}-T}{T_{\mathrm{liquidus}}-T_{\mathrm{solidus}}} & T_{\mathrm{solidus}}\le T\le T_{\mathrm{liquidus}}\\ 1 & T<T_{\mathrm{solidus}}\end{cases} \quad (2)$$

Here, for numerical stability, the phase change was assumed to occur over a small and finite temperature range (T_{liquidus}–T_{solidus}). To ensure that the predicted freezing front is independent of the temperature range, two different temperature ranges of 0.2 °C ($T_{\mathrm{liquidus}} = 0.1$ °C, $T_{\mathrm{solidus}} = -0.1$ °C) and 0.4 °C ($T_{\mathrm{liquidus}} = 0.2$ °C, $T_{\mathrm{solidus}} = -0.2$ °C) were tested. The results showed that prediction results for the two ranges were similar. Therefore, in this study, T_{liquidus} and T_{solidus} were set to be 0.1 °C and −0.1 °C, respectively.

To avoid uncertainties introduced by model parameters, the effective thermal conductivities of foam/water and foam/ice composites were measured separately from the freezing experiments. The experimental setup for effective thermal conductivity measurement was similar to that shown in Fig. 2, except that the top surface of the composite was attached to a heating pad to provide an isoflux boundary condition. The top surface of the heating pad was thermally insulated. Upon measuring the heat flux and the top and bottom wall temperatures, the effective thermal conductivity can be calculated using Fourier's law. The experimentally measured

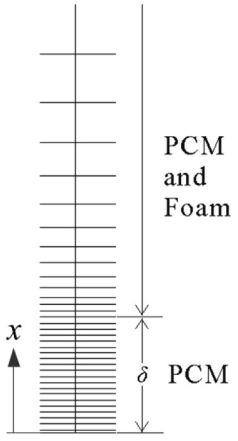

Fig. 5. Theoretical model of one-dimensional freezing of PCMs saturated in metal foam.

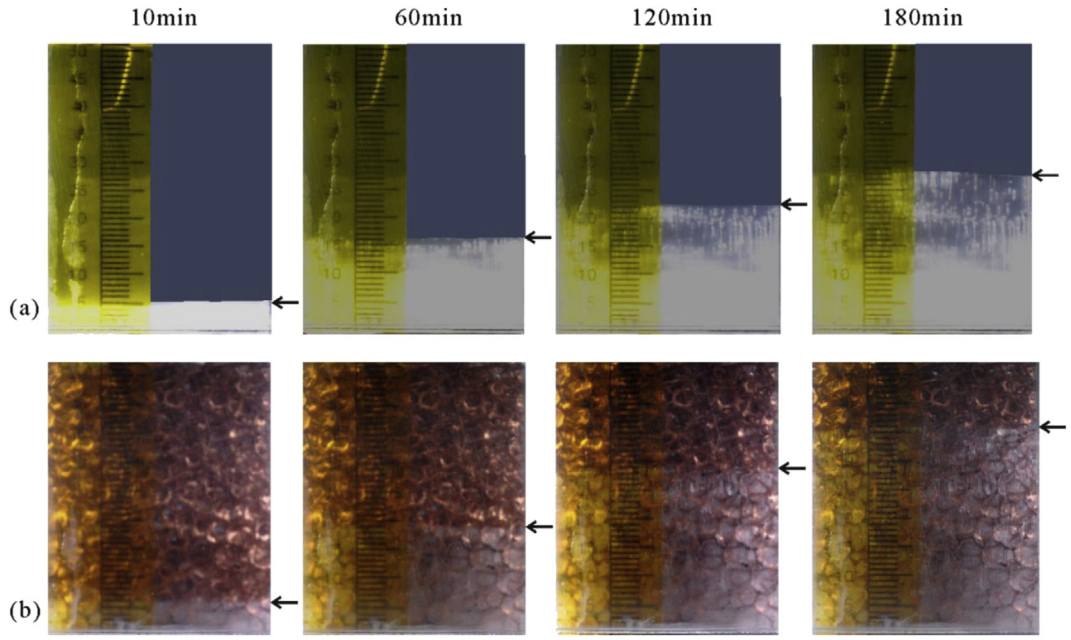

Fig. 6. Evolution of freezing front for pure water: (a) without Metal foam (case 1); and (b) with Copper foam (case 5, sample 2).

effective thermal conductivities of sample 1 and sample 2 are listed in Table 2, along with the thermal properties of water/ice used in the simulation. Note that when eq. (1) was applied to the sub-layer region ($0 \le x \le \delta$), $k_{ef,l}$ and $k_{ef,s}$ should be the thermal conductivities of water and ice, respectively, and the porosity should take the value of 1.

The governing equation was numerically solved using the finite difference method with the following boundary conditions: at $x = 0$, the temperature profile measured on the cold wall as a function of time was specified (as presented in Fig. 7); at $x = H$, an adiabatic thermal boundary condition was applied. The initial temperature was set to be T_i according to the measured value.

4. Results and discussion

4.1. Evolution of the freezing front

Fig. 6(a) and (b) show typical phase distributions for case 1 and case 5, respectively, at 10/60/120/180 min during the freezing process. For both cases, the thickness of the ice layer grew continuously with elapsed time. With cooling from the bottom, the cold (heavy) water is located at the bottom and the warm (light) water is at the top; hence, global natural convection in the water is weak. Consequently, the transfer of heat is dominated by nearly one-dimensional heat conduction with phase change, as indicated by the flat freezing front. However, at a later stage, e.g., $t = 180$ min, for case 1 without metal foam, the thickness of the ice near the side walls of the housing appears to be slightly smaller than that in the central area, see Fig. 6(a). This may be caused by imperfect thermal insulation at the side walls. For case 5 with sample 2, the temperature fields of water/ice are homogenized by the foam *via* heat conduction, thus the freezing front is flatter than in case 1.

Table 2
Thermal properties used in theoretical modelling.

Material	Parameter	Value
Foam (8PPI, $\varepsilon = 0.96$)	Effective thermal conductivity of foam/water, $k_{ef,l}$ (W/mK)	3.47
	Effective thermal conductivity of foam/ice, $k_{ef,s}$ (W/mK)	3.92
Foam (8PPI, $\varepsilon = 0.98$)	Effective thermal conductivity of foam/water, $k_{ef,l}$ (W/mK)	1.95
	Effective thermal conductivity of foam/ice, $k_{ef,s}$ (W/mK)	2.24
Water	Density, $\rho_{PCM,l}$ (kg/m^3)	1000
	Specific heat, $c_{PCM,l}$ (J/kgK)	4216
	Thermal conductivity, $k_{PCM,l}$ (W/mK)	0.56
	Freezing latent heat, L (J/kg)	3.3×10^5
Ice	Density, $\rho_{PCM,s}$ (kg/m^3)	920
	Specific heat, $c_{PCM,s}$ (J/kg K)	2040
	Thermal conductivity, $k_{PCM,s}$ (W/mK)	1.9

4.2. Local thermal equilibrium between foam and PCM

To investigate the local thermal equilibrium, three pairs of thermocouples, *i.e.*, (TC#3, TC#4), (TC#5, TC#6) and (TC#7, TC#8), were used to measure the temperatures of foam and water/ice within the pore at three vertical locations, i.e., $x \approx 10$ mm, 28 mm and 46 mm; see Fig. 2(b). Fig. 7 shows the variation of transient temperatures recorded by TC#3~TC#8 for sample 1. It was found that the temperature of the solid foam ligament was similar to that of water/ice within the nearby pore, indicating that local thermal equilibrium prevails in the investigated metal foam and water PCM

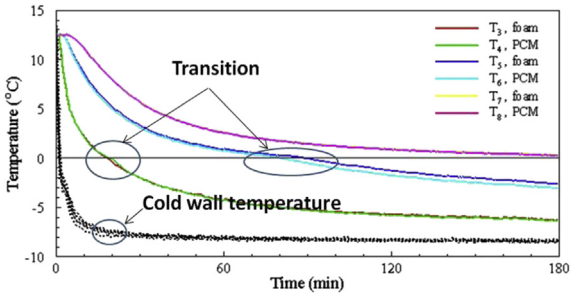

Fig. 7. Experimentally measured temperature variations of copper foam and PCM during freezing.

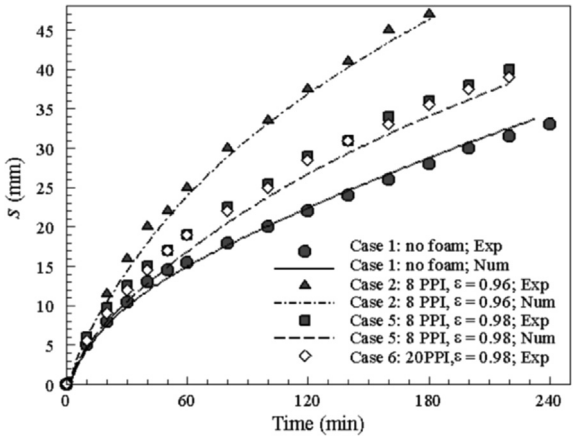

Fig. 8. Growth of ice thickness plotted as a function of elapsed time during freezing for cases 1, 2, 5, and 6 as listed in Table 1.

system. The temperature measured by TC#5 is slightly higher than that measured by TC#6; this is because the bead of TC#5 was located 1.4 mm farther away from the cold wall compared to TC#6.

With supercooling of water ignored during freezing, phase change (solidification) occurs immediately after the temperature drops to the freezing temperature (0 °C). A careful examination of Fig. 7 indicates the transition of the temperature profiles for TC#4 and TC#6 around the freezing temperature (0 °C). As shown in Fig. 7, the slopes of the temperature profiles for TC#4 and TC#6 suddenly increased as the liquid water began to solidify at approximately the freezing temperature, which is a result of the thermal conductivity of ice being ~3 times that of water.

The variation of cold wall temperatures recorded by TC#1 and TC#2 for the six test cases of Table 1 are also included in Fig. 7 (dashed lines). The temperature of the cold wall dropped rapidly before reaching a constant value of −8.4 °C at a time of 30 min after beginning recirculation of the working fluid through the isothermal bath and the CCP. Despite using an isothermal bath, the CCP temperature was not strictly constant throughout the entire freezing process; nevertheless, the cold wall temperatures were consistent for each of the six test cases.

4.3. Effect of metal matrix and foam properties on the freezing rate

For cold thermal energy storage systems, a high freezing rate is usually required to shorten the charging time. In the present study, the freezing rate can be determined by the amount of water solidified in a given amount of time, i.e., by the change in the ice thickness. Fig. 8 plots the growth of ice thickness as a function of elapsed time for cases 1, 2, 5 and 6, with both experimental (symbols) and numerical (lines) results included. Good agreement between experimental and numerical results is observed, suggesting that local thermal equilibrium holds between the foam and PCM because this was assumed in the theoretical model. In Fig. 8, the discrepancies between experimental data and simulation results in cases 2 and 5 may be caused by the error of the effective thermal conductivities adopted in the model.

For case 1, without metal foam, the freezing rate is rather low, especially at later times due to the increasing thermal conduction resistance of the ice layer. In comparison, for the cases with metal foams, a significantly reduced time period was observed to form a given ice thickness. For instance, to form an ice layer with a thickness of 33 mm, case 1 requires a freezing time of 240 min, while the freezing is 156 min and 96 min for the cases with metal foams having a porosity of 0.98 and 0.96, respectively. In other words, upon introducing high porosity metal foams into the water, the required freezing time is reduced by 35% and 60%, respectively. The porosity of metal foam is lower, the heat transfer rate is higher, and thus, the required freezing time is shorter as more conductive material is introduced into the PCM. However, by comparing case 5 and case 6, it was found that pore density has limited influence on the freezing rate, as natural convection in the liquid PCM is negligible and the heat transfer is dominated by heat conduction.

4.4. Effect of contact conditions on the freezing rate

In Fig. 9(a), the experimentally measured growth of ice thickness is plotted as a function of elapsed time for cases 2, 3 and 4. These three cases were tested using the same foam sample but with different contact conditions between the foam and the cold wall. It was found that the influence of contact conditions on the freezing rate was negligible. This finding is verified by the results presented in Fig. 9(b) using the theoretical model, where the worst contact condition (i.e., the foam separated from the cold wall by a gap δ up to 1 mm) was considered. In contrast, for a metal foam/air system, the contact resistance has significant influence on heat transfer [18], as the thermal conductivity of air is two orders of magnitude lower than that of water/ice. The results of Fig. 9 further indicate that when water or other materials with similar thermal conductivity are used as the PCM, it is not necessary to bond the foam to the cold wall *via* sintering, thermal adhesive or other methods. This is practically significant, as considerable cost can be saved for constructing thermal energy storage systems.

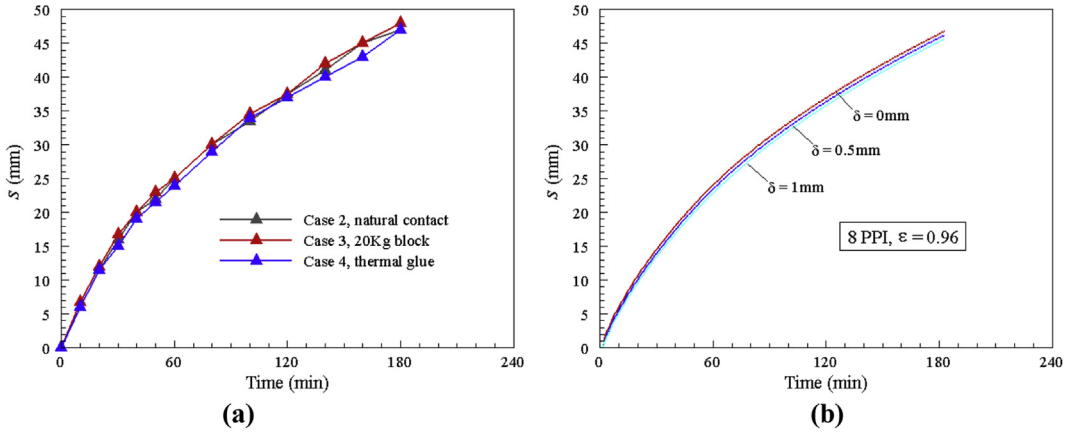

Fig. 9. Effect of contact conditions on freezing rate: (a) Experimental results; (b) Simulation results.

5. Conclusions

Unidirectional freezing of water as PCM saturated in metal foams has been investigated experimentally and theoretically under an isothermal boundary condition. Compared to the case of pure water without metal foams, significant reductions in freezing time, 35% and 60%, were observed by introducing open-cell copper foams with porosities of 0.98 and 0.96, respectively. It was also observed that the pore density (or, equivalently, the pore size) of metal foams has little influence on the freezing rate because the heat transfer is dominated by heat conduction.

The three tested contact conditions (i.e., natural contact, applied pressure, and bonding with a high thermal conductivity adhesive) between the metal foam and cold wall led to similar freezing rates for the investigated copper foam/water PCM system. This indicates that in practice one can simply embed metal foam blocks into PCMs (with similar thermal conductivities as water) with no need of bonding them to the cold wall *via* sintering, a thermal adhesive or other methods.

Local thermal equilibrium between metal foam and water (as PCM) was observed through experimental measurements. It was found that a one-equation model sufficed for modelling the phase change process enhanced by metal foam studied herein.

Acknowledgements

This work was supported by the National Natural Science Foundation of China (51206128), the National Basic Research Program of China (2011CB610305), the National "111" Project of China (B06024), China Postdoctoral Science Foundation Funded Project (2012M521766), Shaanxi Province Science Foundation funded project and the Fundamental Research Funds for the Central Universities of China.

References

[1] E. Oró, A. de Gracia, A. Castell, M.M. Farid, L.F. Cabeza, Review on phase change materials (PCMs) for cold thermal energy storage applications, Appl. Energy 99 (2012) 513–533.
[2] C.Y. Zhao, W. Lu, Y. Tian, Heat transfer enhancement for thermal energy storage using metal foams embedded within phase change materials (PCMs), Sol. Energy 84 (2010) 1402–1412.
[3] L. Fan, J.M. Khodadadi, Thermal conductivity enhancement of phase change materials for thermal energy storage: a review, Renew. Sustain. Energy Rev. 15 (2011) 24–46.
[4] D. Fernandes, F. Pitié, G. Cáceres, J. Baeyens, Thermal energy storage: "How previous findings determine current research priorities", Energy 39 (2012) 246–257.
[5] L. Fan, J.M. Khodadadi, An experimental investigation of enhanced thermal conductivity and expedited unidirectional freezing of cyclohexane-based nanoparticle suspensions utilized as nano-enhanced phase change materials (NePCM), Int. J. Therm. Sci. 62 (2012) 120–126.
[6] S. Wu, D. Zhu, X. Zhang, J. Huang, Preparation and melting/freezing characteristics of Cu/Paraffin nanofluid as phase-change material (PCM), Energy Fuels 24 (2010) 1894–1898.
[7] S. Wu, D. Zhu, X. Li, H. Li, J. Lei, Thermal energy storage behavior of Al_2O_3–H_2O nanofluids, Thermochim. Acta 483 (2009) 73–77.
[8] K.C. Nayak, S.K. Saha, K. Srinivasan, P. Dutta, A numerical model for heat sinks with phase change materials and thermal conductivity enhancers, Int. J. Heat Mass Transf. 49 (2006) 1833–1844.
[9] A. Abhat, Experimental investigation and analysis of a honeycomb-packed phase change material device, in: AIAA 11th Thermophysics Conference, 1976 (Paper AIAA-76–437).
[10] K. Nakaso, H. Teshima, A. Yoshimura, S. Nogami, Y. Hamada, J. Fukai, Extension of heat transfer area using carbon fiber cloths in latent heat thermal energy storage tanks, Chem. Eng. Process. Process Intensif. 47 (5) (2008) 879–885.
[11] L.F. Cabeza, H. Mehling, S. Hiebler, F. Ziegler, Heat transfer enhancement in water when used as PCM in thermal energy storage, Appl. Therm. Eng. 22 (2002) 1141–1151.
[12] C.Y. Zhao, Z.G. Wu, Heat transfer enhancement of high temperature thermal energy storage using metal foams and expanded graphite, Sol. Energy Mater. Sol. Cells 95 (2011) 636–643.
[13] O. Mesalhy, K. Lafdi, A. Elgafy, K. Bowman, Numerical study for enhancing the thermal conductivity of phase change material (PCM) storage using high thermal conductivity porous matrix, Energy Convers. Manag. 46 (2005) 847–867.
[14] Y. Tian, C.Y. Zhao, A numerical investigation of heat transfer in phase change materials (PCMs) embedded in porous metals, Energy 36 (2011) 5539–5546.
[15] W.Q. Li, Z.G. Qu, Y.L. He, W.Q. Tao, Experimental and numerical studies on melting phase change heat transfer in open-cell metallic foams filled with paraffin, Appl. Therm. Eng. 37 (2012) 1–9.
[16] S. Krishnan, J.Y. Murthy, S.V. Garimella, A two-temperature model for solid-liquid phase change in metal foams, J. Heat Transf. 127 (2004) 995–1004.
[17] X. Hu, S.S. Patnaik, Modeling phase change material in micro-foam under constant temperature condition, Int. J. Heat Mass Transf. 68 (2014) 677–682.
[18] T. Fiedler, I.V. Belova, G.E. Murch, Critical analysis of the experimental determination of the thermal resistance of metal foams, Int. J. Heat Mass Transf. 55 (2012) 4415–4420.